Polymer 49 (2008) 3157–3167

Contents lists available at ScienceDirect

Polymer

journal homepage: www.elsevier.com/locate/polymer

Reaction-induced microphase separation in thermosetting blends of epoxy resin with poly(methyl methacrylate)-*block*-polystyrene block copolymers: Effect of topologies of block copolymers on morphological structures

Wenchun Fan, Sixun Zheng*

Department of Polymer Science and Engineering, Shanghai Jiao Tong University, 800 Dongchuan Road, Shanghai 200240, PR China

ARTICLE INFO

Article history:
Received 24 January 2008
Received in revised form 13 April 2008
Accepted 8 May 2008
Available online 15 May 2008

Keywords:
Epoxy thermosets
Block copolymers
Nanostructures and topological structures of block copolymer

ABSTRACT

Polystyrene-*block*-poly(methyl methacrylate) (PS-*b*-PMMA) block copolymers with linear and tetra-armed star-shaped topological structures were synthesized *via* sequential atomic transfer radical polymerization (ATRP). With pentaerythritol tetrakis(2-bromoisobutyrate) as the initiator, the star-shaped block copolymers with two sequential structures (*i.e.*, *s*-PMMA-*b*-PS and *s*-PS-*b*-PMMA) were prepared and the arm lengths and composition of the star-shaped block copolymers were controlled to be comparable with those of the linear PS-*b*-PMMA (denoted as *l*-PS-*b*-PMMA). The block copolymers were incorporated into epoxy resin to access the nanostructures in epoxy thermosets, by knowing that PMMA is miscible with epoxy after and before curing reaction whereas the reaction-induced phase separation occurred in the thermosetting blends of epoxy resin with PS. Considering the difference in miscibility of epoxy with PMMA and/or PS, it is judged that the reaction-induced microphase separation occurred in the systems. The design of these block copolymers allows one to investigate the effect of topological structures of block copolymers on the morphological structures of the thermosets. By means of atomic force microscopy (AFM) and small-angle X-ray scattering (SAXS), the morphology of the thermosets was examined. It is found that the nanostructures were formed in the thermosets containing *l*-PMMA-*b*-PS and *s*-PS-*b*-PMMA block copolymers. It is noted that the long-range order of the nanostructures in the epoxy thermosets containing *l*-PMMA-*b*-PS is obviously higher than that in the system containing *s*-PS-*b*-PMMA. However, the macroscopic phase separation occurred in the thermosetting blends of epoxy resin with *s*-PMMA-*b*-PS block copolymer.

1. Introduction

Study on the morphological structure of thermoset blends is important for the modification of this class of materials [1]. Generally, modifiers of thermosets are some elastomers and thermoplastics. In practice, the thermoset blends are prepared starting from the homogeneous solution composed of precursors of thermoset and the modifiers. With the occurrence of curing reaction, reaction-induced phase separation occurs [1] and fine phase-separated morphologies were obtained. It is recognized that the morphology of multi-component thermosets is quite dependent on the competitive kinetics between the phase separation and polymerization.

In general, the reaction-induced phase separation occurs on the macroscopic scale since some of these modifiers are homopolymers or random copolymers. If block copolymers are used with the presence of miscible blocks, the reaction-induced phase separation could be confined to the nanometer scales and thus the nanostructures were obtained. Recently, it is identified that the formation of ordered or disordered nanostructures in thermosets can greatly optimize the interactions between matrix of thermosets and modifiers and thus the mechanical properties of materials were further improved [2–5]. It should be pointed out that in the thermosets containing amphiphilic block copolymers, the formation of the nanostructures could follow two quite different mechanisms: (i) self-assembly and (ii) reaction-induced microphase separation. Hillmyer et al. [2–15] proposed the self-assembly mechanism to create the nanostructures in thermosets. In this approach, the precursors of thermosets act as the selective solvents of block copolymers and self-organized nanostructures are formed in the mixtures. With adding curing agent to the system the preformed self-assembly microphases can be fixed *via* the curing reactions. In other words, the role of curing reaction is to lock in the morphologies that are already present. The premise of this approach is that self-organized nanostructures must be formed prior to curing. Nonetheless, this case is not always achieved. In many cases, all the subchains of block copolymers are miscible with

* Corresponding author. Tel.: +86 21 54743278; fax: +86 21 54741297.
E-mail address: szheng@sjtu.edu.cn (S. Zheng).

0032-3861/$ – see front matter © 2008 Elsevier Ltd. All rights reserved.
doi:10.1016/j.polymer.2008.05.010

the precursors of thermosets due to the non-negligible entropic contribution (ΔS_m) to free energy of mixing (ΔG_m) since the molecular weights of precursors for thermosets are quite low [1,16]. In addition, the presence of the self-organized structures formed at lower temperatures does not guarantee the survival of the nanostructures at elevated temperatures that are generally required for the preparation of some high performance thermosets since the mixtures of polymers with precursors of thermosets often display the upper critical solution temperature (UCST) behaviors [1,16]. Under this circumstance, it is proposed that the microphase-separated structures can alternatively be accessed *via* the approach of reaction-induced microphase separation, in which the nanostructures are formed by controlling the microphase separation of a part of subchains of block copolymers whereas the other subchains still remain miscible with the crosslinked thermosets [17–26]. Mechanistically, the formation of nanostructures *via* self-assembly is based on the equilibrium thermodynamics in the mixture of precursors of thermosets and amphiphilic block copolymers, which is governed by the nature of precursors of thermosets and block copolymers. Nonetheless, the morphological control *via* the mechanism of reaction-induced microphase separation is quite dependent on the competitive kinetics between polymerization and microphase separation. The approach of reaction-induced microphase separation has not been deeply investigated *vis-a-vis* the self-assembly approach.

During the past years, a variety of block copolymer architectures have been employed to access ordered (or disordered) nanostructures in thermosets. With the synthesis of versatile block -copolymers [27–33], one can have tremendous space for maneuver to control the formation of nanostructures. In ample literature, the formation of ordered and disordered nanostructures was reported by incorporating AB type amphiphilic diblock (and/or ABA type triblock) copolymers into thermosets [2–26]. Nonetheless, the structural effect of block copolymers on the formation of nanostructures in thermosets was occasionally investigated. Rebizant et al. [4,13,14] investigated the ordered nanostructures in epoxy thermosets containing ABC triblock copolymers, *e.g.*, polystyrene-*block*-polybutadiene-*block*-poly(methyl methacrylate). In this system, poly(methyl methacrylate) subchain in the block copolymers remains miscible with epoxy thermosets. Serrano et al. [19,20] reported the formation of the ordered nanostructures in epoxy thermosets while the star-shaped block copolymers (*i.e.*, epoxidized polystyrene-*block*-polybutadiene-*block*-polystyrene) were employed. The epoxide polybutadiene block participated in the formation of crosslinked networks of epoxy resin.

The purpose of this work is to investigate the influence of topological and sequential structures of block copolymers on the formation of nanostructures in epoxy thermosets containing polystyrene-*block*-poly(methyl methacrylate) (PMMA) block copolymers. It has been known that PMMA blocks are miscible with epoxy after and before curing reaction [4,13,14] whereas the reaction-induced microphase separation occurs in the thermosetting blends of epoxy resin and polystyrene [21,26]. It is expected that if any, the formation of the microscopic (and/or macroscopic) phase separation structures will follow the mechanism of reaction-induced demixing. Toward this end, we design to synthesize three block copolymers with different topological structures (linear *versus* star-shaped) and sequential structures of blocks. Linear poly-(methyl methacrylate)-*block*-polystyrene (*l*-PMMA-*b*-PS) and tetra-armed PMMA-*b*-PS diblock copolymers with PMMA (and/or PS) subchains connected core molecules were synthesized *via* sequential atomic transfer radical polymerization (ATRP). For the sake of comparison, the lengths of PS (and/or PMMA) subchains in block copolymers are identical. In this work, atomic force microscopy (AFM) and small-angle X-ray scattering (SAXS) are used to examine the disordered or ordered nanostructures formed *via* the reaction-induced microphase separation. The difference in nanostructures for the epoxy thermosets has been addressed on the basis of the restriction of topological structure of block copolymers on the formation of nanophases.

2. Experimental

2.1. Materials

Diglycidyl ether of bisphenol A (DGEBA) with epoxide equivalent weight of 185–210 was purchased from Shanghai Resin Co., China. The curing agent is 4,4′-methylenebis-(2-chloroaniline) (MOCA), supplied by Shanghai Reagent Co., China.

Both styrene (St) and methyl methacrylate (MMA) are of analytically pure grade and were purchased from Shanghai Reagent Co., China. Prior to use, the inhibitor was removed by washing with aqueous NaOH (5 wt%) and deionized water for at least three times and dried by anhydrous Mg_2SO_4; the monomers were further distilled at reduced pressure. 2-Bromoisobutyryl bromide, ethyl-2-bromoisobutyrate and *N*,*N*,*N*′,*N*′,*N*″-pentamethyldiethylenetriamine (PMDETA) were purchased from Aldrich Co., USA and used as received. Copper(I) bromide (CuBr) was obtained from Shanghai Reagent Co., China and it was purified according to the reported procedure [34]. Pentaerythritol was supplied by Shanghai Reagent Co., China and its purification was carried out *via* sublimation at reduced pressure. Triethylamine (TEA) was of analytically pure grade and was dried over CaH_2 and then was refluxed with *p*-toluenesulfonyl chloride followed by distillation. All the solvents used in this work are obtained from commercial resources and were purified according to standard procedures.

2.2. Synthesis of pentaerythritol tetrakis(2-bromoisobutyrate)

Pentaerythritol tetrakis(2-bromoisobutyrate) was synthesized by following the procedure reported by Matyjaszewski et al. [35]. Typically, to a 250 ml round-bottom flask, 3.70 g (27.0 mmol) pentaerythritol and 12.0 g (0.12 mol) triethylamine and 100 ml tetrahydrofuran (THF) were charged. A solution composed of 26.0 g (0.12 mol) 2-bromoisobutyryl bromide and 40 ml tetrahydrofuran (THF) was dropwise added with a pressure equalizing addition funnel in the atmosphere of highly pure nitrogen at 0 °C. At this temperature, the reaction was carried out overnight and then the system was heated up to room temperature. The white solids were obtained *via* recrystallization from diethyl ether solution with the yield of 41% (8.0 g). By means of DSC, the melting point (M_p) was measured to be 133–134 °C. ^{1}H NMR ($CDCl_3$, ppm): 4.31 [s, 8H, C–CH_2–O], 1.93 [s, 24H, C(Br)–CH_3].

2.3. Synthesis of linear and star-shaped macroinitiators

For the synthesis of linear poly(methyl methacrylate) (PMMA) macroinitiators, to a 50 ml round-bottom flask, mono-functional initiators, ethyl 2-bromoisobutyrate (0.2338 g, 1.4 mmol), CuBr (0.1008 g, 0.7 mmol), PMDETA (146 μl, 0.7 mmol), anisole (7.0 ml) and MMA (14.0 g, 0.14 mol) were charged. Connected to a standard Schlenk line system, the reactive system was degassed *via* three pump–freeze–thaw cycles and then immersed in a thermostated oil bath at 90 °C. The polymerization was carried out for 1.5 h and the system was cooled to room temperature. The solvent, THF, was added to dissolve the product. After passed over a column of neutral alumina, the solution was concentrated and then dropped into an excessive amount of cold methanol to afford the precipitates. The polymer of 10.4 g was obtained with the monomer conversion of 72.6%.

To synthesize star-shaped polystyrene (PS) macroinitiators, to a 50 ml round-bottom flask, pentaerythritol tetrakis(2-bromoisobutyrate) (0.2762 g, 0.38 mmol), CuBr (0.217 g, 1.5 mmol), PMDETA

Table 1
Molecular weights of macroinitiators and block copolymers

Samples	M_n[a]	M_n/arm[a]	M_w/M_n[a]	R[b]
Linear PMMA macroinitiator	7400	7400	1.25	–
Star-shaped PMMA macroinitiator	32,300	7900	1.20	–
Star-shaped PS macroinitiator	26,400	6400	1.12	–
l-PMMA-*b*-PS	12,700	–	1.34	0.53
s-PS-*b*-PMMA	61,600	15,400	1.42	0.47
s-PMMA-*b*-PS	57,600	14,400	1.35	0.50

[a] Calculated by gel permeation chromatography.
[b] R denotes the content of PS subchain of the block copolymers determined by ^{1}H NMR spectroscopy.

(313 μl, 1.5 mmol), anisole (12 ml) and styrene (15.737 g, 0.15 mol) were charged. Connected to the Schlenk line system, the reactive system was degassed *via* three pump–freeze–thaw cycles and then immersed in a thermostated oil bath at 110 °C. The polymerization was carried out for 2.5 h and the system was cooled to room temperature. The solvent, THF, was added to dissolve the product. After passed over a column of neutral alumina, the solution was concentrated and then dropped into an excessive amount of cold methanol to afford the precipitates. After drying in a vacuum oven at room temperature for 24 h, 9.8 g linear PS macroinitiator was obtained with a monomer conversion of 60.5%. For the synthesis of star-shaped poly (methyl methacrylate) (PMMA) macroinitiators, to a round-bottom flask, pentaerythritol tetrakis(2-bromoisobutyrate) (0.2928 g, 0.4 mmol), CuBr (0.0864 g, 0.6 mmol), PMDETA (125 μl, 0.6 mmol), anisole (20 ml) and MMA (24 g, 0.24 mol) were charged. The similar procedures of synthesis and purification were used as the synthetic procedure of star-shaped PS macroinitiators. The polymerization was allowed to perform at 90 °C for 3.5 h and 12.7 g polymer was obtained with a monomer conversion of 51.6%. The molecular weights of the polymer were measured by means of gel permeation chromatography and the results are summarized in Table 1.

2.4. Synthesis of block copolymers

To synthesize the block copolymers with different architectures by atomic transfer radical polymerization (ATRP), the above macroinitiators were used. For the synthesis of *l*-PMMA-*b*-PS, to a flask connected with the standard Schlenk line system, the linear PMMA macroinitiators (M_n (GPC) = 7500, 2.0 g, 0.27 mmol), CuBr (0.0417 g, 0.27 mmol), PMDETA (63.9 μl, 0.27 mmol), anisole (6.0 ml), and styrene (6.0 g, 0.0576 mol) were charged. The reactive mixture was degassed *via* three pump–freeze–thaw cycles and then immersed in a thermostated oil bath at 110 °C. After the polymerization was carried out for 12 h, the system was cooled to room temperature. The solvent, THF, was added to dissolve the product. After passed over a column of neutral alumina, the solution was concentrated and then dropped into an excessive amount of cold methanol to afford the precipitates. The precipitates were obtained and dried in a vacuum oven at room temperature for 24 h. The *l*-PMMA-*b*-PS diblock copolymer was obtained with the styrene conversion of 23.4% (3.4 g).

The syntheses of the tetra-armed star-shaped block copolymers (*i.e.*, *s*-PMMA-*b*-PS and *s*-PS-*b*-PMMA) were carried out through the similar procedures. The ATRP of styrene and methyl methacrylate was initiated with the star-shaped poly(methyl methacrylate) (PMMA) and polystyrene (PS) macroinitiators, respectively. To keep the length of block and composition of the block copolymers identical with the linear diblock copolymers (*l*-PMMA-*b*-PS), the desired conversions of the monomers were carefully controlled. All the block copolymers were subjected to the measurements by gel permeation chromatography (GPC). It is noted that the profiles of GPC show that each polymer displays a unimodal distribution of molecular weight distribution. The molecular weights of the polymers were measured by means of gel permeation chromatography and the results are summarized in Table 1.

2.5. Preparation of epoxy thermosets containing block copolymers

The block copolymers with various topological structures (*i.e.*, *l*-PMMA-*b*-PS, *s*-PS-*b*-PMMA and *s*-PMMA-*b*-PS) were added to DGEBA at ambient temperature with continuous stirring until the homogenous and transparent mixtures were obtained. After that, MOCA was added to systems with vigorous stirring until homogeneous blends were obtained. The ternary mixtures were poured into Teflon moulds and cured at 150 °C for 2 h plus 180 °C for 2 h to access a complete curing reaction. The thermosetting blends containing block copolymers up to 40 wt% were prepared.

2.6. Measurement and characterization

2.6.1. Nuclear magnetic resonance (NMR) spectroscopy

The diblock copolymers were dissolved in deuterated chloroform, and the ^{1}H NMR spectra were measured on a Varian Mercury Plus 400 MHz NMR spectrometer with tetramethylsilane (TMS) as the internal reference.

2.6.2. Gel permeation chromatography (GPC)

The molecular weights of polymers were determined on a Waters 717 Plus autosampler gel permeation chromatography apparatus equipped with Waters RH columns and a Dawn Eos (Wyatt Technology) multi-angle laser light scattering detector and the measurements were carried out at 25 °C with tetrahydrofuran (THF) as the eluent at the rate of 1.0 ml/min.

2.6.3. Scanning electron microscopy (SEM)

In order to observe the morphology of the samples, the thermosets were fractured under cryogenic condition using liquid nitrogen. The fractured surfaces so obtained were immersed in THF at room temperature for 30 min. In the thermosetting blends, thermoplastic phases (if any) could be preferentially etched by the solvent while epoxy matrix phase remains unaffected. The etched specimens were dried to remove the solvents. The fracture surfaces were coated with thin layers of gold of about 100 Å. The thermosets containing linear PMMA and *s*-PMMA-*b*-PS were examined with a Hitachi S210 scanning electron microscope (SEM) at an activation voltage of 15 kV while the thermosets containing *l*-PMMA-*b*-PS were observed by means of a JEOL JSM 7401F field emission scanning electron microscope (FESEM) at an activation voltage of 5 kV.

2.6.4. Atomic force microscopy (AFM)

The specimens of thermosets for AFM observation were trimmed using a microtome machine, and the thickness of the specimens was about 70 nm. The morphological observation of the samples was conducted on a Nanoscope IIIa scanning probe microscope (Digital Instruments, Santa Barbara, CA) in a tapping mode. A tip fabricated from silicon (125 μm in length with ca. 500 kHz resonant frequency) was used for scanning. Typical scan speeds during recording were 0.3–1.0 line s^{-1} using scan heads with a maximum range of 16 μm × 16 μm.

2.6.5. Small-angle X-ray scattering (SAXS)

The SAXS measurements were taken on a Bruker Nanostar system. Two-dimensional diffraction patterns were recorded using an image intensified CCD detector. The experiments were carried out at room temperature (25 °C) using CuKα radiation ($\lambda = 1.54$ Å, wavelength) operating at 40 kV, 35 mA. The intensity profiles were output as the plot of scattering intensity (I) *versus* scattering vector, $q = (4/\lambda)\sin(\theta/2)$ (θ = scattering angle).

3. Results and discussion

3.1. Synthesis of block copolymers

The synthetic routes of the block copolymers with various topological structures, *i.e.*, *l*-PMMA-*b*-PS, *s*-PS-*b*-PMMA and *s*-PMMA-*b*-PS are summarized in Scheme 1. The sequential atomic transfer radical polymerization (ATRP) was employed to obtain the block copolymers. Firstly, the linear and/or star-shaped macroinitiators (*i.e.*, *s*-PS and *s*-PMMA) were synthesized through ATRP, which were initiated with ethyl-2-bromoisobutyrate and pentaerythritol tetrakis(2-bromoisobutyrate), respectively. Pentaerythritol tetrakis(2-bromoisobutyrate) was prepared *via* the reaction between pentaerythritol and 2-bromoisobutyryl bromide in the presence of triethylamine. Shown in Fig. 1 is the ^{1}H NMR spectrum of pentaerythritol tetrakis(2-bromoisobutyrate). The resonance at 1.93 ppm is assigned to the protons of methyl groups and that at 4.31 to the protons of methylene groups of this compound. By controlling the conversion of the monomers (*i.e.*, MMA and St), the macroinitiators with the desired molecular weights were obtained, which was measured with GPC. The macroinitiators were further used to initiate the polymerization of St and MMA to afford the block copolymers with various topological structures. Shown in Fig. 2 are the ^{1}H NMR spectra of *l*-PMMA-*b*-PS, *s*-PS-*b*-PMMA and *s*-PMMA-*b*-PS block copolymers together with the assignment of these spectra. The ratio of the integration intensity of protons in the aromatic rings (7.01–6.52 ppm) of PS block to the protons of methoxy groups (at 3.60 ppm) of PMMA block can be used to estimate the composition of block copolymers. The contents of PS block of these copolymers determined in terms of ^{1}H NMR spectra together with the molecular weights of the macroinitiators and the results are summarized in Table 1. It is noted that for the three samples of block copolymers, the ratios of subchains (*i.e.*, PMMA and PS) and the arm length of the star-shaped block copolymers are comparable with those of the linear PMMA-*b*-PS diblock copolymers.

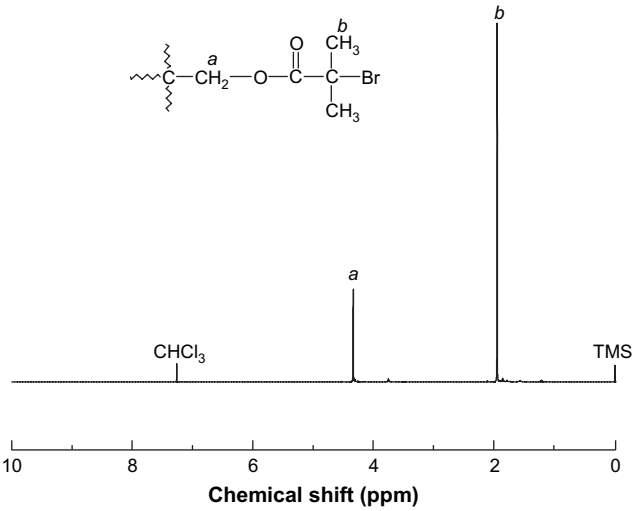

Fig. 1. ^{1}H NMR spectrum of pentaerythritol tetrakis(2-bromoisobutyrate).

3.2. Miscibility of binary thermosetting blends of epoxy with PMMA (and/or PS)

The knowledge of the miscibility and phase behavior in the thermosetting blends of epoxy with PS (and/or PMMA) is important for one to understand the formation of microstructures in the thermosets containing the diblock copolymers. For the blends of epoxy with PS, it has been known that before curing, the mixtures of the precursor of epoxy thermoset (*e.g.*, DGEBA) displayed an upper critical solution temperature (UCST) behavior [21]. It is noted that for the binary mixture of DGEBA with the model PS with the molecular weight comparable with that of the PS subchain of the block copolymers used in this work, the UCST is only 85 °C, which is quite lower than 150 °C (*i.e.*, the curing temperature). The experimental fact implies that the curing of epoxy blends would start from the homogenous mixtures. Upon adding the curing agent (*viz.*, MOCA) to the system, the thermosetting blends of epoxy with PS

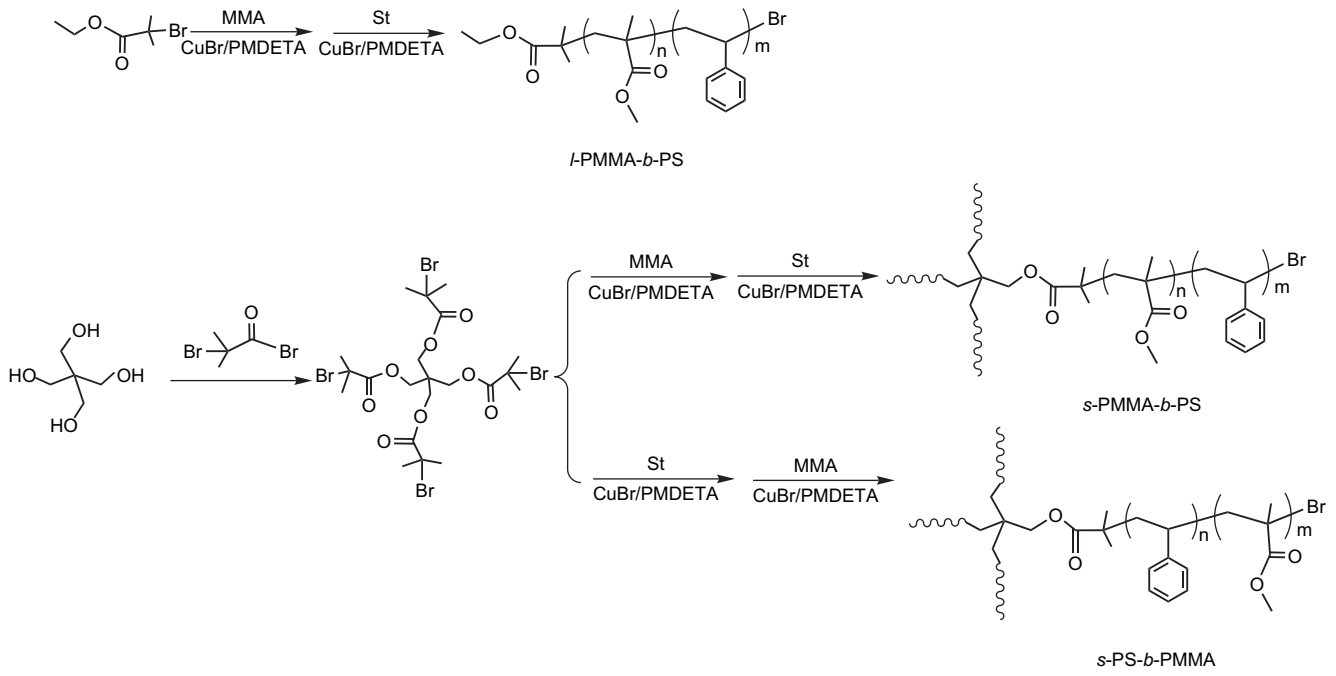

Scheme 1. Synthesis of *l*-PMMA-PS, *s*-PMMA-*b*-PS and *s*-PS-*b*-PMMA block copolymers.

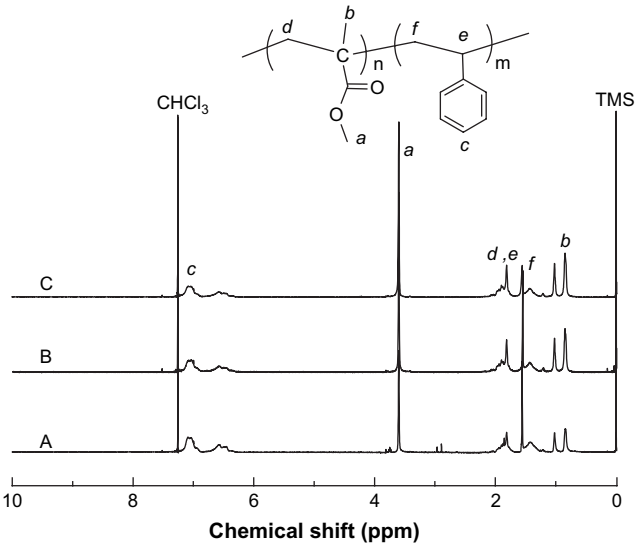

Fig. 2. ^{1}H NMR spectra of (A) *l*-PMMA-*b*-PS, (B) *s*-PS-*b*-PMMA and (C) *s*-PMMA-*b*-PS.

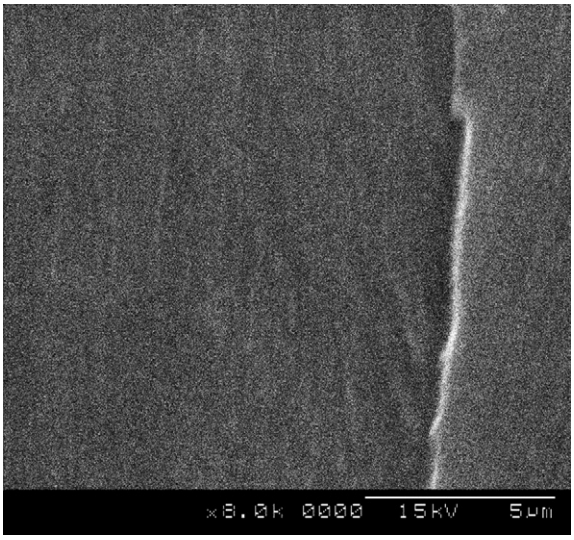

Fig. 3. SEM micrograph of the epoxy thermosetting blend containing 20 wt% PMMA. The fracture end of the blend has been etched with tetrahydrofuran for 30 min.

were obtained after cured at 150 °C for 2 h plus 180 °C for 2 h to access a complete curing reaction. It was observed that with the curing reaction proceeding, the initially homogeneous and transparent mixtures gradually became cloudy, indicating that the reaction-induced phase separation occurred [1].

It is imperative to investigate the miscibility in the thermosetting blends of epoxy and PMMA. Toward this work, the model PMMA with the molecular weight identical with the length of PMMA subchains in the linear or star-shaped PMMA-*b*-PS diblock copolymers was prepared. Before curing, all the mixtures composed of DGEBA, MOCA and PMMA are homogenous and transparent at room and elevated temperatures. This observation, PMMA is miscible with the precursors of epoxy thermosets. After cured at 150 °C for 4 h, the ternary miscible mixtures were gradually converted into the binary blends of thermosets. The miscibility was further verified by scanning electron microscopy (SEM). The SEM micrograph of the blend containing 20 wt% PMMA is representatively shown in Fig. 3. Before morphological observation, the fractured ends of the specimen were etched for 30 min with the solvent of PMMA. It is expected that PMMA phase would be rinsed whereas epoxy matrix remains unaffected if the reaction-induced phase separation occurred in the blends. Nonetheless, it is seen that after etched the homogeneous morphology was still obtained. This observation indicates that PMMA is miscible with epoxy thermosets. The miscibility of epoxy and PMMA blends cured with MOCA is in an agreement with the observation for epoxy and PMMA blends cured with 4,4′-methylene-[3-chloro 2,6-diethylanilene] (MCDEA) by Ritzenthaler et al. [9,10].

3.3. Morphology of thermosets containing block copolymers

The above block copolymers with various topological structures were incorporated into epoxy thermosets. Before curing, all the mixtures of the precursors of epoxy with the block copolymers are homogenous and transparent, suggesting that no macroscopic phase separation occurred. This observation is in accordance with the complete miscibility of precursors of epoxy (*i.e.*, DGEBA and MOCA) with PMMA (and/or PS). All the blends of thermosets containing the diblock copolymers were prepared by curing at 150 °C for 2 h plus 180 °C for 2 h to access a complete curing reaction.

3.3.1. Thermosets containing l-*PMMA*-b-*PS diblock copolymers*

Except for the thermoset containing *l*-PMMA-*b*-PS diblock copolymer of 40 wt%, all the cured blends were homogenous and transparent, indicating that no macroscopic phase separation occurred. The thermoset containing 40 wt% *l*-PMMA-*b*-PS is translucent. The epoxy thermosets containing *l*-PMMA-*b*-PS were subjected to the morphological observation by means of atomic force microscopy (AFM). The AFM micrographs of the thermosets containing 10, 20, 30, and 40 wt% of the *l*-PMMA-*b*-PS are presented in Fig. 4. Shown in the left-hand side of each micrograph is the topography image and in the right is the phase image. It is seen that the thermosetting blends containing the linear block copolymer less than 40 wt% exhibited nanostructured morphologies. In terms of the volume fraction of PS in the thermosets, it is plausible to propose that the continuous matrix is attributed to the crosslinked epoxy, which could be miscible with PMMA subchains of the diblock copolymer, while the light region is responsible for PS domains. For the thermoset containing 10 wt% *l*-PMMA-*b*-PS, the PS spherical nanoparticles with the size of 50–60 nm in diameter were homogeneously dispersed into the continuous epoxy matrix. With increasing the content of the block copolymer, some interconnected PS microdomains began to appear (Fig. 4C) and the quantity of the PS microdomains was increased, whereas the size of the spherical particle remains almost invariant (Fig. 4A–C). It is of interest to note that corona-like microdomains with the size of ~100 nm were observed for the thermoset containing 40 wt% *l*-PMMA-*b*-PS (Fig. 4D). It is seen that the spherical PS nanoparticles were surrounded by a layer with the thickness of 20 nm. It is proposed that the external layer of PS nanodomains is formed from the demixing of PMMA subchains induced by polymerization. In the binary thermosetting blends of epoxy resin with PMMA, the PMMA chains can be homogeneously dispersed into the epoxy matrix and were well interpenetrated into the crosslinked epoxy networks. In contrast, the PMMA chains have to be enriched at the surface of the microphase-separated PS nanodomains due to the presence of chemical bonds between PS and PMMA subchains in the blends. Due to the steric hindrance, the PMMA chains at the intimate surface of PS nanodomains could not be well mixed with epoxy matrix. This phenomenon that the miscible subchains were demixed from the thermosetting matrix upon curing has been reported in the self-assembly of epoxy resin and amphiphilic block copolymer nanocomposites [3–14].

The formation of the nanostructures in the thermosets containing *l*-PMMA-*b*-PS diblock copolymer was further investigated by means of small-angle X-ray scattering (SAXS). Shown in Fig. 5 are the SAXS profiles of the thermosets containing 10, 20, 30,

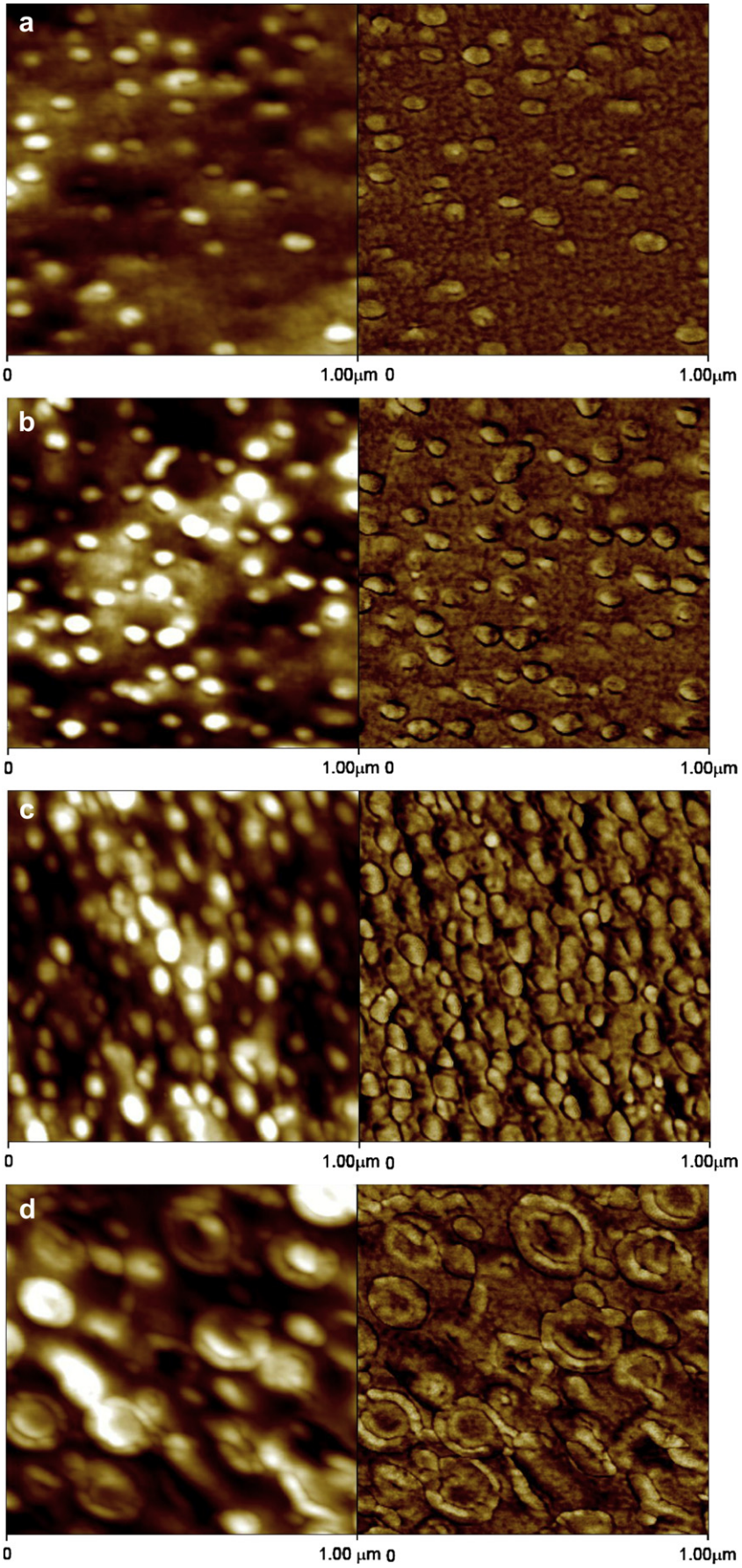

Fig. 4. AFM images of the thermosets containing (A) 10, (B) 20, (C) 30, and (D) 40 wt% of *l*-PMMA-*b*-PS diblock copolymer. Left: topography; right: phase contrast images.

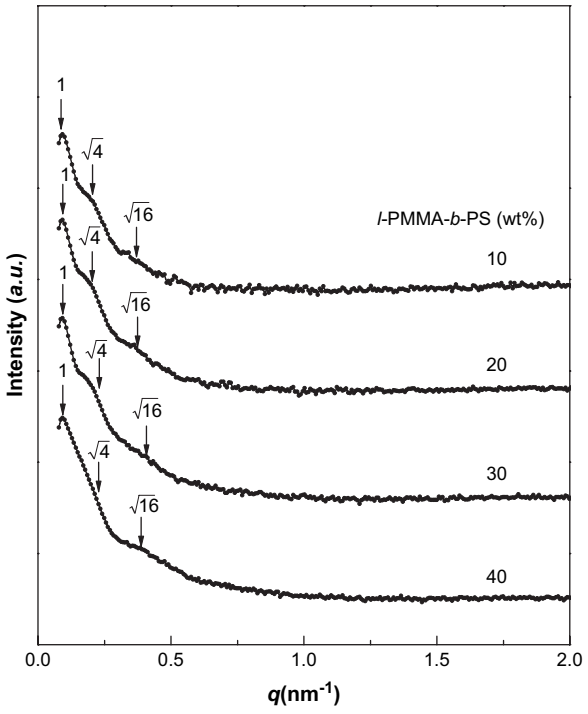

Fig. 5. SAXS profiles of the thermosets containing *l*-PMMA-*b*-PS diblock copolymer. Each profile has been shifted vertically for clarity.

40 wt% of *l*-PMMA-*b*-PS diblock copolymer. The well-defined scattering peaks were observed in all the cases, indicating that the thermosets containing *l*-PMMA-*b*-PS are microphase-separated. It is noted that all the SAXS profiles exhibited the multiple scattering maxima as denoted by the arrows on each curve, indicating that the thermosets could possess long-range ordered microstructures. The scattering peaks of the thermosets are situated at the q values of 1, $4^{0.5}$ and $16^{0.5}$ relative to the first-order scattering peak positions (q_m), which suggests that these are lattice scattering peaks of spherical (or cylindrical) nanophases arranged in cubic lattices such as body-centered cubic (bcc), face-centered cubic (fcc) and simple cubic symmetries. In addition, hexagonally packed cylindrical morphology is also possible. It should be pointed out that it is not easy unambiguously to judge the type of packing lattices only in terms of SAXS profiles for the thermosetting blends containing 10, 20, 30 wt% *l*-PMMA-*b*-PS copolymer because the scattering peaks are quite broad, *i.e.*, the ordering is apparently not good enough.

3.3.2. Thermosets containing star-shaped block copolymers

The star-shaped diblock copolymers (*i.e.*, *s*-PMMA-*b*-PS and *s*-PS-*b*-PMMA) with the different sequence of blocks were synthesized with the identical composition of copolymers. The length of arm for the block copolymer stars is close to the molecular weight of *l*-PMMA-*b*-PS diblock copolymer. The star-shaped block copolymers are incorporated into epoxy to investigate the effect of topological structures of block copolymers on the morphology of thermosets.

Before curing, all the mixtures composed of DGEBA, MOCA and or *s*-PS-*b*-PMMA (and/or *s*-PMMA-*b*-PS) were homogenous and transparent, indicating that no macroscopic phase separation occurred at the scale exceeding the wavelength of visible light. After cured with the condition identical with the preparation of the blends containing *l*-PMMA-*b*-PS, the thermosetting blends containing *s*-PS-*b*-PMMA and *s*-PMMA-*b*-PS were, respectively, obtained. It is seen that the thermosets containing *s*-PS-*b*-PMMA block copolymer are homogenous and transparent whereas those containing *s*-PMMA-*b*-PS are white and cloudy. The clarity indicates that no phase separation occurred at the scale exceeding the wavelength of visible light in the epoxy thermosets containing *s*-PS-*b*-PMMA block copolymer whereas macroscopic phase separation induced by reaction took place in the blends of epoxy with *s*-PMMA-*b*-PS. The morphology of the epoxy thermosets containing *s*-PS-*b*-PMMA block copolymer was examined by means of AFM and SAXS. Shown in Fig. 6 are the AFM micrographs of the thermosets containing *s*-PS-*b*-PMMA up to 40 wt%. It is seen that all the thermosets are microphase-separated. In the epoxy thermoset containing 10 wt% *s*-PS-*b*-PMMA, the irregular PS nano-objects are homogeneously dispersed into the continuous epoxy matrix. With increasing the content of *s*-PS-*b*-PMMA block copolymers, some interconnected PS microdomains began to appear (Fig. 6B and C). The thermosets containing 40 wt% *s*-PS-*b*-PMMA diblock copolymer displayed a combined morphology from worm-like to lamellar nano-objects.

The morphologies of the thermosetting blends were further investigated by small-angle X-ray scattering (SAXS). Fig. 7 presents the SAXS profiles of the samples. It is seen that the well-defined scattering peaks at the value of $q = 0.15\ \mathrm{nm}^{-1}$ were observed in all the cases, indicating that the thermosets are microphase-separated. This result is in a good agreement with the observation with AFM. According to the position of the primary scattering peaks, the average distance ($L = 2\pi/q_m$) between the neighboring domains can be estimated to be 60.9, 49.8, 43.3 and 63.1 nm for the thermosetting blends containing 10, 20, 30 and 40 wt% *s*-PS-*b*-PMMA, respectively. Except for the thermoset containing 40 wt% *s*-PS-*b*-PMMA block copolymer, the average distance between the neighboring domains slightly decreased with increasing the content of *s*-PS-*b*-PMMA. This result is in a good agreement with that determined by AFM images Fig. 6A–C. It was seen that the value of L increased up to 63.1 nm while the content of *s*-PS-*b*-PMMA is 40 wt%. This observation is responsible for the transition of nanostructure from worm-like nano-objects in the blend with 30 wt% *s*-PS-*b*-PMMA to lamellar nanostructure in the blend with 40 wt% *s*-PS-*b*-PMMA, which is confirmed by the AFM results (Fig. 6D). It should be pointed out that only single scattering maximum was clearly detected in the SAXS profiles of the thermosets containing *s*-PS-*b*-PMMA, suggesting that the period (or order) of the PS nanodomains arranged in the thermosets containing *s*-PS-*b*-PMMA block copolymer is obviously lower than that in the thermosets containing *l*-PMMA-*b*-PS diblock copolymer.

The morphology of the thermosets containing *s*-PMMA-*b*-PS block copolymer was examined by means of AFM and scanning electronic microscopy (SEM). The SEM micrographs of the blend are shown in Fig. 8. The heterogeneous morphologies at the micrometer scale were observed in all cases. For the blend containing 10 wt% *s*-PMMA-*b*-PS, some irregular particles of the star-shaped block copolymer at the size of 0.3–1.0 μm were dispersed into the continuous epoxy matrix after the fracture ends were etched with the solvent (*e.g.*, THF). For the blend containing 20 wt% *s*-PMMA-*b*-PS, the phase-inverted morphology was displayed after the star-shaped block copolymer was etched with THF. The irregular particles after etched are ascribed to the crosslinked epoxy whereas the continuous body that was rinsed by the solvent is attributed to the star-shaped block copolymer. It is seen that the spherical particles at the scale of several micrometers are dispersed in the continuous matrix of the block copolymer. The morphological structure was further confirmed by means of atomic force microscopy (AFM). Shown in Fig. 9 are the AFM images of thermosetting blend containing 20 wt% *s*-PMMA-*b*-PS. The left and right are the images of height and phase, respectively. The macroscopic phase separation is also observed in the thermosetting blends, which is in a good agreement with the observation by means of SEM.

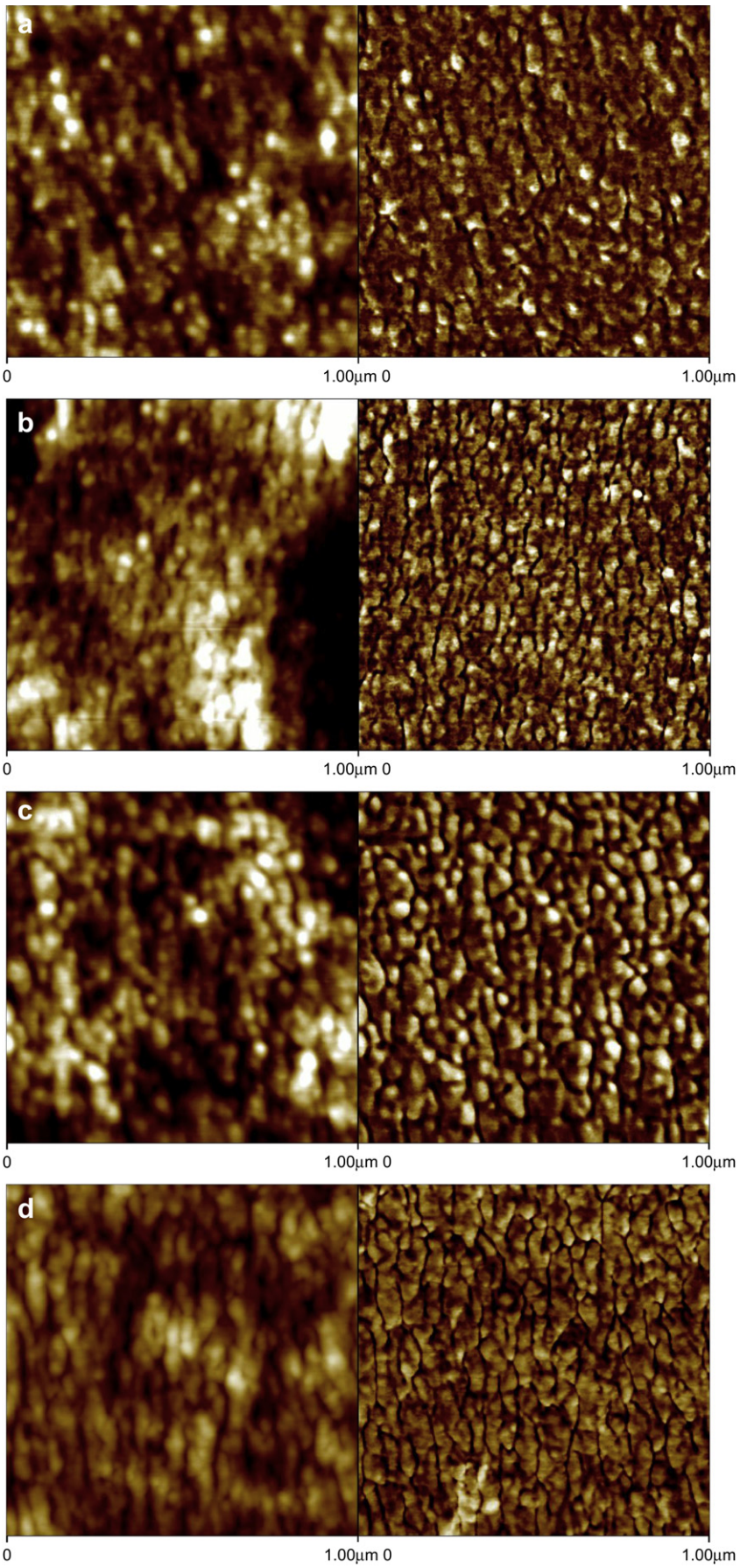

Fig. 6. AFM images of the thermosets containing (A) 10, (B) 20, (C) 30, and (D) 40 wt% of *s*-PS-b-PMMA block copolymer. Left: topography; right: phase contrast images.

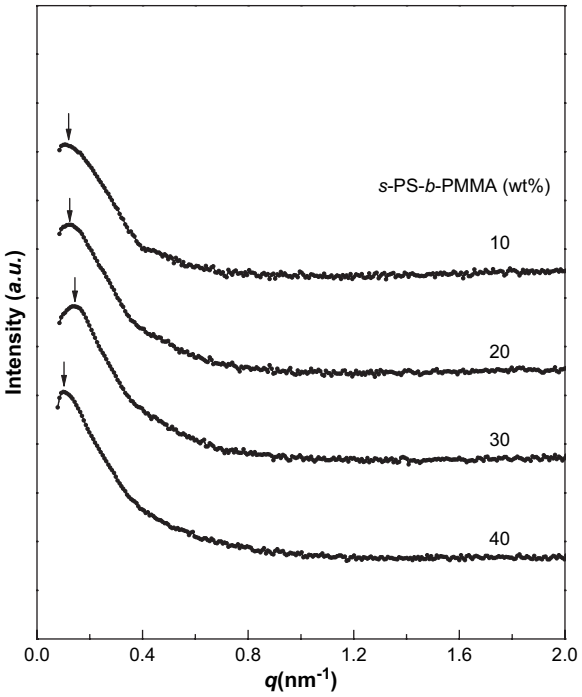

Fig. 7. SAXS profiles of the thermosets containing *s*-PS-b-PMMA block copolymer. Each profile has been shifted vertically for clarity.

It should be pointed out that the present phase-separated structure is quite different from the fine morphology of the thermosetting blends with homopolymers (or random copolymers) *via* reaction-induced polymerization [1]. It is proposed that in the present case the presence of the miscible subchains of the star-shaped block copolymers (*i.e.*, PMMA block), which were directly connected with the core, could restrict the formation of the fine microphase-separated morphology.

3.4. Interpretation of morphological structures

The formation of nanostructures in thermosets containing amphiphilic block copolymers has been reported, which could follow self-assembly [3–14] or reaction-induced microphase separation mechanisms [17–26]. In the present case, the block copolymers (*viz.*, *l*-PMMA-*b*-PS, *s*-PMMA-*b*-PS and *s*-PS-*b*-PMMA) were exploited to access the nanostructures of the epoxy thermosets. It has been known that PMMA is miscible with epoxy after and before curing reaction [9,10] whereas the binary mixtures composed of PS and DGEBA displayed an upper critical solution temperature (UCST) behavior [21–26]. Nonetheless, differential scanning calorimetry (DSC) shows that the ternary mixtures composed of DGEBA, MOCA and PMMA-*b*-PS block copolymers are miscible, which is in marked contrast to the case of the binary mixtures of DGEBA and PS. The miscibility behavior of the ternary mixtures could result from the changes in solubility parameter due to the addition of MOCA. Therefore, it is judged that in the present case the formation of heterogeneous morphology would follow the reaction-induced microphase separation other than self-assembly mechanism.

In this work, the sequential atom transfer radical polymerization (ATRP) was employed to prepare these block copolymer with the identical composition and the impact of the topologies of block copolymers on the morphological structures of the resulting thermoset blends was examined. It is of interest to note that the nanophases in the epoxy thermosets containing *l*-PMMA-*b*-PS were arranged into the ordered lattices such as body-centered cubic (bcc), face-centered cubic (fcc) or simple cubic lattices while the nanodomains in the thermosets containing *s*-PS-*b*-PMMA were packed into lamellar nanostructures. The fact that the less ordered nanostructures were formed in the epoxy thermosets containing *s*-PS-*b*-PMMA could result from the confinement of the star-shaped topology of the diblock copolymer on the reaction-induced microphase separation (see Scheme 2).

Before the curing reaction, the *l*-PMMA-*b*-PS diblock copolymer was fully miscible with the precursors of epoxy thermoset. With the occurrence of the curing reaction, the PS subchains were gradually separated out where the PMMA subchains remained miscible with the epoxy matrix. Due to the presence of the miscible PMMA subchains, the macroscopic phase separation of PS chains was suppressed and only the nanoscopic domains can be formed. The PS nanodomains with the narrow size distribution were packed into ordered (*i.e.*, body-centered cubic (bcc), face-centered cubic (fcc) or simple cubic) lattices. The topological structure of the *s*-PS-*b*-PMMA block copolymer can be taken as the case that the ends of PS subchains of every four *l*-PMMA-*b*-PS macromolecular chains are "wrapped" into a "nodule". In other words, the PS blocks were

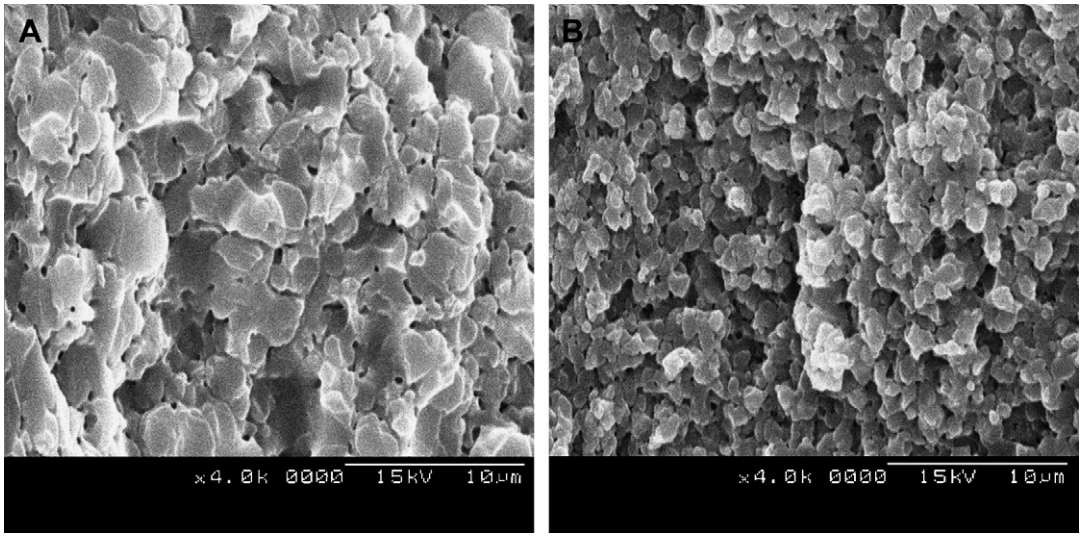

Fig. 8. SEM micrograph of the epoxy thermosetting blend containing *s*-PMMA-*b*-PS. The fracture end of the blend has been etched with tetrahydrofuran for 30 min. (A) 10 wt% *s*-PMMA-*b*-PS and (B) 20 wt% *s*-PMMA-*b*-PS.

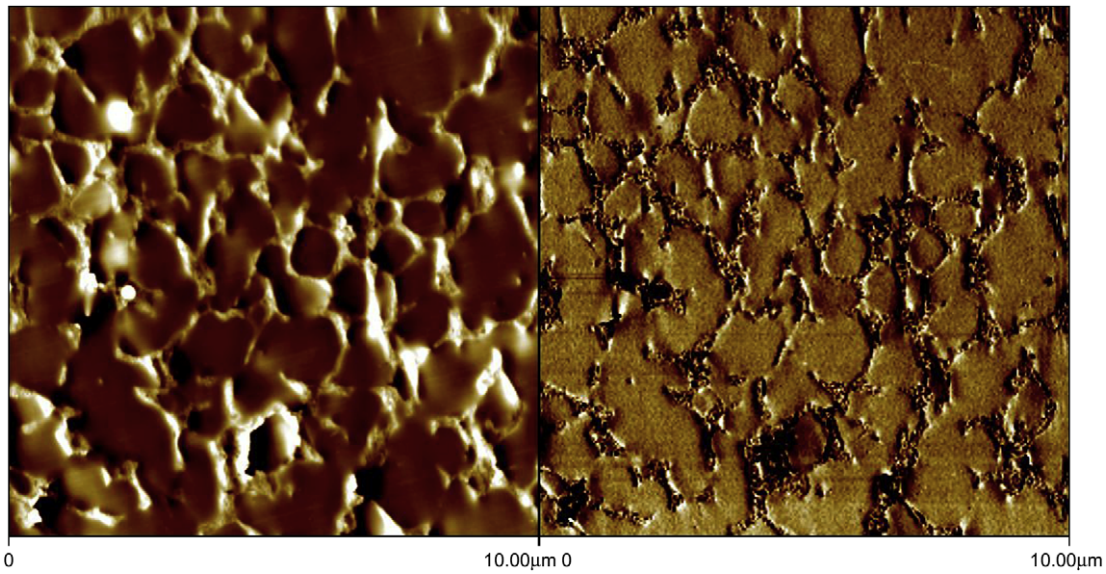

Fig. 9. AFM images of the thermosets containing 20 wt% of *s*-PMMA-*b*-PS block copolymer. Left: topography; right: phase contrast images.

combined into a tetra-armed PS star, the molecular weight of which is four times that of PS subchain in *l*-PMMA-*b*-PS diblock copolymer. Although the *s*-PS-*b*-PMMA block copolymer is also miscible with the precursors of epoxy resin, its mixing entropy with epoxy resin before curing reaction is significantly decreased compared to the *l*-PMMA-*b*-PS diblock copolymer. In addition, the higher molecular weight for PS blocks results so that the upper critical solution temperature (UCST) [21] of the blends of DGEBA with PS block will shift to higher temperature. It is plausible to propose that the decreased entropy of mixing and higher UCST together with the star-shaped topology of PS block give rise to the formation of lamellar nanostructures rather than spherical PS nanodomains. This effect could be taken as the restriction of star-shaped topology of the block copolymer on the formation of the ordered nanostructures.

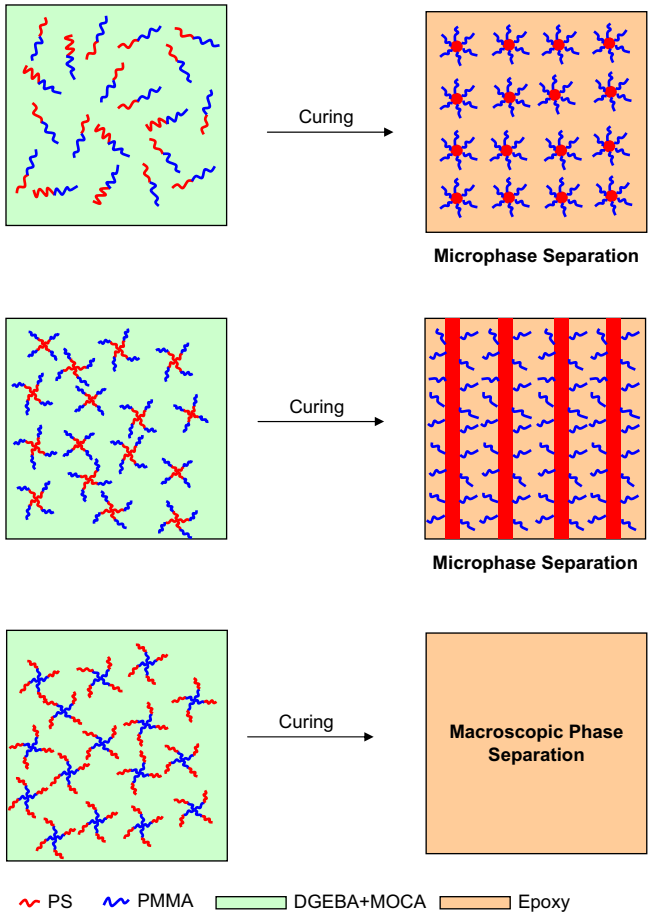

Scheme 2. Formation of phase-separated morphology in epoxy thermosets containing PMMA-*b*-PS block copolymers.

In addition to the effect of topological structures of block copolymers on the morphologies of the resulting thermosets, the subchain sequence of star-shaped block copolymers has a profound influence on the formation of nanostructures in the thermosetting blends. It is of interest to note that with the identical composition and molecular weights of block copolymers, the macroscopic phase separation was observed in the thermosetting blends of epoxy thermosets containing *s*-PMMA-*b*-PS star-shaped block copolymer. This observation can be taken as the effect of sequential structures of star-shaped block copolymer on the morphology of thermosets containing block copolymers, which is responsible for the specific architecture of *s*-PMMA-*b*-PS. In the star-shaped block copolymer, the every four PMMA blocks was covalently connected to one point of branch [*i.e.*, pentaerythritol tetrakis(2-bromoisobutyrate)], *i.e.*, the four PMMA arms were combined into a tetra-armed star-shaped "giant" block, which was surrounded by the immiscible blocks (*viz.* PS). The molecular weight of the tetra-armed star-shaped "giant" PMMA block is four times that of PMMA block in *l*-PMMA-*b*-PS diblock copolymer. Compared to its linear counterpart, the mixing entropy of the mixtures of the *s*-PMM-*b*-PS block copolymer with epoxy before curing reaction is significantly decreased due to the increased molecular weight of the block copolymer. On the other hand, the thermodynamic interactions between epoxy matrix and PMMA could be significantly increased (*i.e.*, the intermolecular interactions are reduced) due to the formation of the tetra-armed star-shaped topological structure of the PMMA subchains [36–43]. In addition, the formation of star-shaped topological structure of the miscible PMMA blocks would ineffectively reduce the surface energy of PS nanodomains, which is in marked contrast to the case of the thermosetting blends containing *l*-PMMA-*b*-PS diblock copolymer. The above factors result in the macroscopic phase separation induced by reaction as in

the thermosetting blending systems containing homopolymers or random copolymers [44–51].

It should be pointed out that the difference in the morphologies of the epoxy thermosets containing different block copolymers with the identical composition could be also associated with some kinetic factors in addition to the above interpretation according to thermodynamics. Each arm of the star-shaped block copolymers (*viz. s*-PS-*b*-PMMA and *s*-PMMA-*b*-PS) has the identical length and composition with *l*-PS-*b*-PMMA (or *s*-PMMA-*b*-PS). Therefore, the molecular weights of the block copolymers are four times that of *l*-PMMA-*b*-PS. The difference in molecular weights could exert some significant influence on viscosity, rheokinetics of microphase separation and viscoelasticity of microphase, *etc.* in the *in situ* polymerization blending systems and thus the morphological structures of blends were affected. This observation is in marked contrast to the formation of nanostructures in the epoxy thermosets containing the *l*-PS-*b*-PMMA with the comparable length of the blocks (*e.g.*, PMMA and PS).

4. Conclusion

Polystyrene-*block*-poly(methyl methacrylate) (PS-*b*-PMMA) block copolymers with linear and tetra-armed star-shaped topological structures were synthesized *via* sequential atomic transfer radical polymerization (ATRP). By controlling the direct connection of the subchains to core, the star-shaped block copolymers with two sequential structures (*i.e.*, *s*-PMMA-*b*-PS and *s*-PS-*b*-PMMA) were prepared. The arm lengths of the star-shaped block copolymers were controlled to be comparable with the molecular weight of the linear PS-*b*-PMMA diblock copolymers and the compositions of the star-shaped block copolymers are identical with their linear homologue (*i.e.*, *l*-PMMA-*b*-PS). The design of the block copolymers allows one to investigate the effect of topological structures of block copolymers on the morphological structures. It is found that the nanostructures were formed in the thermosets containing *l*-PMMA-*b*-PS and *s*-PS-*b*-PMMA block copolymers. Considering the difference in miscibility of epoxy with PMMA and/or PS, it is judged that the reaction-induced microphase separation occurred in the systems. Nonetheless, there is morphological difference between the two blending systems. It is noted that the long-range order of the nanostructures in the epoxy thermosets containing *l*-PMMA-*b*-PS is obviously higher than that in the system containing *s*-PS-*b*-PMMA. The formation of the morphological difference has been interpreted on the basis of the effects of topological structure of the miscible subchains (*i.e.*, PMMA) on the surface free energy of PS nanodomains. However, the phase separation at the scale of micrometer occurred in the thermosetting blends of epoxy resin with the *s*-PMMA-*b*-PS block copolymer. This observation could be responsible for the insufficient suppression of the PMMA chains of macroscopic phase separation of the tetra-armed PS at shell in the block copolymer.

Acknowledgments

The financial supports from Natural Science Foundation of China (No. 20474038) are acknowledged. The authors thank Shanghai Leading Academic Discipline Project (Project Number: B202) for the partial support.

References

[1] Pascault JP, Williams RJJ. In: Paul DR, Bucknall CB, editors. Polymer blends, vol. 1. New York: Wiley; 2000. p. 379–415.
[2] Hillmyer MA, Lipic PM, Hajduk DA, Almdal K, Bates FS. J Am Chem Soc 1997; 119:2749.
[3] Lipic PM, Bates FS, Hillmyer MA. J Am Chem Soc 1998;120:8963.
[4] Dean JM, Verghese NE, Pham HQ, Bates FS. Macromolecules 2003;36:9267.
[5] Wu J, Thio YS, Bates FS. J Polym Sci Part B Polym Phys 2005;43:1950.
[6] Mijovic J, Shen M, Sy JW, Mondragon I. Macromolecules 2000;33:5235.
[7] Guo Q, Thomann R, Gronski W. Macromolecules 2002;35:3133.
[8] Guo Q, Thomann R, Gronski W. Macromolecules 2003;36:3635.
[9] Ritzenthaler S, Court F, Girard-Reydet E, Leibler L, Pascault JP. Macromolecules 2002;35:6245.
[10] Ritzenthaler S, Court F, Girard-Reydet E, Leibler L, Pascault JP. Macromolecules 2003;36:118.
[11] Kosonen H, Ruokolainen J, Nyholm P, Ikkala O. Macromolecules 2001;34: 3046.
[12] Grubbs RB, Dean JM, Broz ME, Bates FS. Macromolecules 2000;33:9522.
[13] Rebizant V, Abetz V, Tournihac T, Court F, Leibler L. Macromolecules 2003;36: 9889.
[14] Rebizant V, Venet AS, Tournillhac F, Girard-Reydet E, Navarro C, Pascault JP, et al. Macromolecules 2004;37:8017.
[15] Zucchi IA, Galante MJ, Williams RJJ. Polymer 2005;46:2603.
[16] Flory PJ. Principles of polymer chemistry. Ithaca, NY: Cornell University Press; 1953.
[17] Larrañaga M, Gabilondo N, Kortaberria G, Serrano E, Remiro PM, Riccardi CC, et al. Polymer 2005;46:7082.
[18] Meng F, Zheng S, Zhang W, Li H, Liang Q. Macromolecules 2006;39:711.
[19] Serrano E, Tercjak A, Kortaberria G, Pomposo JA, Mecerreyes D, Zafeiropoulos NE, et al. Macromolecules 2006;39:2254.
[20] Serrano E, Larrañaga M, Remiro PM, Mondragon I. Macromol Rapid Commun 2005;26:982.
[21] Meng F, Zheng S, Li H, Liang Q, Liu T. Macromolecules 2006;39:5072.
[22] Meng F, Zheng S, Liu T. Polymer 2006;47:7590.
[23] Sinturel C, Vayer M, Erre R, Amenitsch H. Macromolecules 2007;40:2532.
[24] Ocando C, Serrano E, Tercjak A, Pena C, Kortaberria G, Calberg C, et al. Macromolecules 2007;40:4068.
[25] Xu Z, Zheng S. Macromolecules 2007;40:2548.
[26] Meng F, Xu Z, Zheng S. Macromolecules 2008;41:1411.
[27] Lodge TP. Macromol Chem Phys 2003;204:265.
[28] Vasilev C, Reiter G, Pispas S, Hadjichristidis N. Polymer 2006;47(14):330.
[29] Weiser M-S, Thomann Y, Heinz L-C, Pasch H, Muehaupt R. Polymer 2006; 47(12):4505.
[30] Das S, Yilgor I, Yilgor E, Inci B, Tezgel O, Beyer FL, et al. Polymer 2007;48(10): 290.
[31] Xiong H, Zheng JX, Van Horn RM, Jeong K-U, Quirk RP, Lotz B, et al. Polymer 2007;48(8):3732.
[32] Siegwart DJ, Wu W, Mandalaywala M, Tamir M, Sarbu T, Silverstein MS, et al. Polymer 2007;48(5):7279.
[33] Pietsch T, Gindy N, Fahmi A. Polymer 2008;49(3):914.
[34] Wang J-S, Matyjaszewski K. J Am Chem Soc 1995;117:5614.
[35] Matyjaszewski K, Miller PJ, Pyun J, Kichelbick G, Diamanti S. Macromolecules 1999;32:6526.
[36] Faust AB, Sremcich PS, Gilmer JW, Mays JW. Macromolecules 1989;22: 1250.
[37] Greenberg CC, Foster MD, Turner CM, Corona-Galvan S, Coutet E, Butler PD, et al. Polymer 1999;40:4713.
[38] Fredrickson GH, Liu AJ, Bates FS. Macromolecules 1994;27:2503.
[39] Grayce CJ, Schweizer KS. Macromolecules 1995;28:7461.
[40] Greenberg CC, Foster MD, Turner CM, Corona-Galvan S, Coutet E, Quirk RP, et al. J Polym Sci Part B Polym Phys 2001;39:2549.
[41] Martter TD, Foster MD, Ohno K, Hassleton DM. J Polym Sci Part B Polym Phys 2002;40:1074.
[42] Martter TD, Foster MD, Yoo T, Xu S, Lizarraga G, Quirk RP. J Polym Sci Part B Polym Phys 2003;41:247.
[43] Lee JS, Foster MD, Wu DT. Macromolecules 2006;39:5113.
[44] Yamanaka K, Inoue T. Polymer 1989;30:662.
[45] Yee AF, Pearson RA. Polym Mater Sci Eng 1990;63:311.
[46] Inoue T. Prog Polym Sci 1995;20:119.
[47] Zheng S, Hu Y, Guo Q, Wei J. Colloid Polym Sci 1996;274:410.
[48] Zheng S, Wang J, Guo Q, Wei J, Li J. Polymer 1997;37:4667.
[49] Francis B, Thomas S, Jose J, Ramaswamy R, Rao VL. Polymer 2005;46:12372.
[50] Poel GV, Goossens S, Goderis B, Groeninckx G. Polymer 2005;46:10758.
[51] Francis B, Rao VL, Poel GV, Posada F, Groeninckx G, Ramaswamy R, et al. Polymer 2006;47:5411.